

The nature and age of Mesoproterozoic strike-slip faulting based on Re-Os geochronology of syn-tectonic copper mineralization, Assynt Terrane, NW Scotland

R. E. Holdsworth^{1,2}, D. Selby^{1,3}, E. Dempsey⁴, L. Scott¹, K. Hardman¹, A.E. Fallick⁵, R. Bullock¹

1 = Department of Earth Sciences, Durham University, Durham DH1 3LE, UK

2 = Geospatial Research Ltd, Durham DH1 4EL, UK

3 = State Key Laboratory of Geological Processes and Mineral Resources, School of Earth Resources, China University of Geosciences, Wuhan, 430074, Hubei, China.

4 = Department of Geography, Environment and Earth Sciences, University of Hull, Hull HU6 7RX, UK

5 = SUERC, Scottish Enterprise Technology Park, Rankine Avenue, East Kilbride G75 0QF, UK

**Corresponding author (e-mail: r.e.holdsworth@durham.ac.uk)*

Abstract:

In ancient basement regions such as the Lewisian Complex, NW Scotland, the ages of brittle deformation events are commonly poorly constrained due to a lack of datable fills. An array of NW-SE sinistral and antithetic E-W dextral faults related to a regionally recognized episode of brittle shearing cut Neoproterozoic gneisses and c. 2.25 Ga quartz-pyrite veins close to the trace of the unexposed, regional-scale NW-SE fault. Copper-iron mineralisation occurs at an intersection between an antithetic dextral fault and an older c. 2.25 Ga quartz vein. Optical microscopy, SEM and XRD analyses reveal an array of intergrown, co-genetic copper-iron sulphides, hematite and barite. Complex mm-thick zoned alteration rims rich in epidote occur at contacts between the sulphides and gneisses. Rhenium-Osmium copper-iron sulphide geochronology yields an age of c. 1.55 Ga for the hydrothermal mineralization event associated with faulting. Fault movements demonstrably overlap with mineralisation based on the asymmetric fibrous growth forms of these minerals within local dextral shears which acted as local channelways for mineralizing fluids during and after faulting. We tentatively propose that this regionally recognised strike slip faulting, previously termed the 'Late Laxfordian', should be referred to as the 'Assyntian' in order to distinguish it from kinematically distinct Laxfordian events. **[end]**

31 The Neoarchaean gneisses of the Lewisian Complex in NW Scotland form a well exposed and relatively
32 accessible area of Laurentian continental basement rocks that lie in the immediate foreland region of the
33 Palaeozoic Caledonian Orogen (Wheeler *et al.* 2010). The metamorphic gneisses preserve evidence for
34 several tectonic events each formed under different P-T conditions (MacDonald *et al.* 2015; Park 2005).
35 The superimposition of multiple ductile and brittle deformation events, in addition to several episodes of
36 metamorphism, mineralisation, hydrothermal alteration, and igneous intrusion have generated a complex
37 deformational fabric. The Lewisian Complex therefore represents a good opportunity to study a wide
38 array of geological processes that occur through deep geological time.

39 Cross-cutting and overprinting relationships observed in the field and thin section are traditionally
40 used in basement complexes to allow relative age relationships to be established on both regional and
41 local scales. Only radiometric ages, however, are able to give information concerning the absolute ages of
42 events. Despite the emergence of an increasing number of geochronometers, the relative scarcity of
43 material suitable for reliable radiometric dating remains a significant problem, particularly for the later
44 brittle and brittle-ductile phases of deformation. Since such events can form over periods spanning many
45 hundreds of million years, this means that a large part of the geological history is poorly constrained. More
46 specifically, a lack of absolute age data has become somewhat problematic in Scotland ever since Kinny
47 *et al.* (2005) and Friend & Kinny (2001) proposed that the Lewisian Complex may comprise a number of
48 lithologically and geochronologically distinct tectonic units (fault/shear zone-bounded terranes)
49 assembled progressively during a series of Precambrian amalgamation episodes perhaps spanning more
50 than a billion years.

51 This paper describes a hitherto little studied set of epidote mineralized NW-SE sinistral and
52 antithetic E-W dextral brittle faults which cut the Neoarchaean Lewisian gneisses, Palaeoproterozoic mafic
53 dykes, and quartz-pyrite veins in part of the Assynt Terrane close to the NW-SE-trending regional scale

54 Loch Assynt Fault (Figs 1a-c). Rhenium-Osmium geochronology on associated syn-tectonic copper-iron
55 sulphide mineralization is used to provide an absolute age for the brittle-ductile shearing deformation for
56 the first time. This permits tentative correlation with other regional events in nearby regions of Baltica
57 and Laurentia. In addition to advances in our understanding of deformation in continental cratons, the
58 present paper also demonstrates the value of the Re-Os technique for dating Proterozoic-age sulphide
59 mineralisation events.

60 **Regional setting**

61 The Precambrian rocks of the Lewisian Complex, NW Scotland form a fragment of the continental
62 basement of Laurentia that lies to the west of the mid-Silurian Caledonian Moine Thrust (Fig. 1a). The
63 rocks are largely unaffected by Caledonian deformation and have experienced a number of much older
64 crustal-scale geological events during the Neoarchaeon and Palaeoproterozoic. The Lewisian Complex is
65 divided into a number of tectonic regions or terranes which are predominantly separated by steeply-
66 dipping shear zones or faults (Fig. 1a; e.g. Park 2002, 2005).

67 The Assynt Terrane (Fig. 1b) forms the central part of the Lewisian Complex in mainland NW
68 Scotland. It comprises grey, banded, tonalite–trondjemite–granodioritic (TTG) gneisses which are locally
69 highly heterogeneous lithologically, and also include distinct units of mafic-ultramafic composition (e.g.
70 Sheraton *et al.* 1973; Guice *et al.* 2018). The TTG gneisses are thought to be derived from igneous plutons
71 intruded at *c.* 3.03–2.96 Ga (high precision U-Pb and Sm-Nd geochronology; Hamilton *et al.* 1979; Friend
72 & Kinny 1995; Kinny & Friend 1997). These rocks then underwent deformation and granulite facies
73 metamorphism during the so-called Badcallian event(s) the timing of which is incompletely resolved with
74 current age constraints suggesting either a more widely favoured age of *c.* 2.76 Ga (e.g. Corfu *et al.* 1994;
75 Zhu *et al.* 1997; MacDonald *et al.* 2015), and/or a younger age of *c.* 2.49–2.48 Ga (e.g. Friend & Kinny
76 1995; Kinny & Friend 1997).

77 The central part of the Assynt Terrane is cut by the c. 1.5 km wide, NW-SE-trending, steeply dipping
78 dextral transpressional Canisp Shear Zone (CSZ; Attfield 1987; Fig. 1a). There are also many other smaller
79 steeply-dipping, NW-SE to WNW-ESE trending minor shear zones cutting the surrounding Badcallian
80 gneisses (Park & Tarney 1987) including the Stoer Shear Zone. Some of these shear zones are thought to
81 have developed initially during Inverian deformation and amphibolites-facies retrogression which
82 affected substantial parts of the Assynt Terrane (Attfield 1987). The absolute age of this event is also
83 somewhat unclear, with a majority of studies considering it to be c. 2.4 Ga (e.g. Corfu *et al.* 1994; Love *et*
84 *al.* 2004; Goodenough *et al.* 2013). The Badcallian and Inverian structures are cross-cut by a regionally
85 extensive set of NW-SE trending mafic and ultramafic intrusions referred to as the Scourie Dyke Swarm
86 (Fig. 1b). Individual intrusions range in thickness from a few millimetres to several tens of metres and
87 were intruded as two suites of differing age: a dominant c. 2.42-2.38 Ga set and a more minor group at c.
88 2.0 Ga (Rb-Sr whole rock and U-Pb geochronology; Chapman 1979; Heaman & Tarney 1989; Davies &
89 Heaman 2014). These dykes display evidence of having been emplaced under amphibolite facies pressures
90 and temperatures, i.e. in the middle crust, possibly immediately following the Inverian event (O'Hara
91 1961; Tarney 1973; Wheeler *et al.* 2010).

92 In the Assynt and Gruinard terranes (Fig. 1a), the dykes and older structures in the host rock gneisses
93 are cross cut by a regional set of quartz-pyrite veins emplacement of which has been dated using Re-Os
94 geochronology at c. 2.26 Ga (Vernon *et al.* 2014). These veins, and the older structures, are all
95 heterogeneously overprinted by younger Laxfordian deformation with widespread retrogression of the
96 TTG gneisses under lower amphibolite to upper greenschist-facies metamorphic conditions (e.g. Sutton &
97 Watson 1950; Attfield 1987; Beacom *et al.* 2001). The regionally recognised Laxfordian begins with a series
98 of magmatic events c. 1.9–1.87 Ga – at least some of which are related to island arc development –
99 followed by a protracted orogenic episode lasting from 1.79 to 1.66 Ga (see discussion in Goodenough *et*
100 *al.* 2013). The effects of Laxfordian reworking in the Assynt Terrane are highly localised, being largely

101 restricted to the central 1 km wide centre of the CSZ and other, narrower local shear zones, as well as
102 along the margins of the Scourie dykes. This contrasts with the Rhiconich and Gruinard Terranes which lie
103 respectively NE and SW of the Assynt Terrane (Fig. 1a), where the Laxfordian event reached amphibolite
104 facies and was associated with more pervasive ductile shearing and reworking (Droop *et al.* 1989). This
105 led to the suggestion that the Assynt Terrane represents a shallower depth crustal block during the
106 Laxfordian (e.g. Dickinson & Watson 1976; Coward & Park 1987).

107 In both the Assynt and Gruinard terranes, a younger set of sinistral low greenschist-facies mylonitic
108 shear zones, brittle faults and localised folds is recognised developed sub-parallel to the pre-existing high-
109 strain fabrics in Laxfordian and Inverian shear zones, and the margins of some Scourie dykes (Beacom *et al.*
110 *al.* 2001). These structures are informally referred to as the 'Late Laxfordian' and are thought to include
111 the initial development of the regional scale Loch Assynt Fault (Fig. 1b; cf. Krabbendam & Leslie 2010).
112 The precise age of the 'late-Laxfordian' faulting is poorly constrained, but in the Assynt Terrane these
113 structures demonstrably pre-date deposition of the unmetamorphosed and little deformed c. 1.2 Ga
114 Torridonian Stoer Group (Beacom *et al.* 2001). This suggests that the presently exposed parts of the
115 Lewisian Complex had been exhumed to the surface by that time. Regionally, both the Stoer Group and
116 the Lewisian Complex are in turn unconformably overlain by younger Torridonian sequences (Diabeg and
117 Torridon groups) thought to have been deposited no earlier than 1.04 Ga (Park *et al.* 1994).

118 The present study focusses on a small region of copper sulphide mineralisation, which is found
119 spatially associated with quartz veins and faults cutting Lewisian gneisses on a small island linked to the
120 N shore of Loch Assynt when water levels are low (NC2127 2497, Figs 2a, b). The occurrence of copper
121 mineralisation is rarely described in the Assynt Terrane and has only been briefly referred to at localities
122 near to the Bay of Clachtoll (Boyd & Crichton 1960) and at Loch an Eisg-brachaidh (MacLeod in Boyd &

123 Crichton 1960). We were unable to locate the occurrence of such mineralization at those locations during
124 the present study.

125 **Field and laboratory methods**

126 *Fieldwork, sampling and petrography*

127 Fieldwork studied faults and associated mineralization cutting Lewisian gneisses and Scourie dykes
128 exposed along or close to the shores of Loch Assynt (Figs 2a, b) where the water level – and therefore
129 ease of access to the outcrop - varies dependent on recent rainfall patterns. The relative ages of country
130 rock fabrics, igneous intrusions, mineral veins and fault rocks were ascertained from observed cross
131 cutting relationships. Structural geometries were recorded through collection of orientation data; brittle
132 fault kinematics were determined based on offsets of markers in the host rocks, local preservation of
133 slickenline lineations and preservation of asymmetric brittle shear criteria such as en-echelon veins and
134 slickenline steps (Petit 1987). A representative sample set of orientated hand specimens were collected
135 from country rocks, fault rocks and mineral veins and were used to study microstructures and the timing
136 of mineralization relative to deformation. Both reflected and transmitted light optical microscopy, and
137 scanning electron microscopy (BSEM) were used to study the composition and microstructural
138 characteristics of the copper and associated mineralization. Having identified and removed appropriate
139 material for dating, Re-Os geochronology was used to determine the age of copper-iron sulphide
140 mineralisation and sulphur isotope composition to constrain the mineralizing fluid origin.

141

142 *Rhenium-Osmium geochronology analytical methods*

143 The copper mineralization comprises of co-genetic intergrown copper sulphides (55%, anilite, djurleite in
144 roughly equal amounts), copper-iron sulphides (40%, bornite) and minor supergene alteration products
145 (5%, malachite, covellite) (see below). Given the intimate micron-scale intergrowth textures, a pure
146 monomineralic separate could not be achieved. A bulk copper sulphide mineral separate (0.5 g) was

147 therefore taken from an area with only minor evidence of the supergene minerals covellite and malachite.
148 Given that our petrographic observations suggest that all the sulphide phases are co-genetic, we suggest
149 that an analysis of a single relatively unaltered bulk sample of copper mineralization is justified. Optical
150 light microscope observation of the obtained 70-200 mesh fraction mineral indicates that the separate
151 was 90% copper-iron sulphides with the remaining 10% comprising intergrown hematite > barite >
152 malachite > covellite. The Re-Os analysis was performed at the Durham Geochemistry Centre in the Arthur
153 Holmes and Source Rock and Sulphide Geochemistry and Geochronology laboratories using the protocols
154 outlined in Selby *et al.* (2009) and Vernon *et al.* (2014). Briefly, the sulphide mineral separate (0.4 g)
155 together with a known amount of mixed $^{190}\text{Os} + ^{185}\text{Re}$ tracer solution and a 1:2 mix of inverse *aqua-regia*
156 (3 mL 11N HCl and 6 mL 15N HNO_3) were loaded and sealed into a Carius tube, and heated to 220°C for
157 48 hours. Osmium was purified from acidic solution using solvent (CHCl_3) and micro-distillation methods.
158 From the Os extracted acidic solution, Re was isolated using solvent extraction (NaOH-acetone) and anion
159 chromatography. The purified Re and Os fractions were loaded onto Ni and Pt wire filaments respectively,
160 with the isotope compositions determined using a Triton Thermo Scientific Mass Spectrometer. Rhenium
161 isotopes were measured statically using Faraday Collectors, with the Os measured in peak hopping mode
162 using the Secondary Electron Multiplier. All data are blank corrected using a total procedural blank run
163 alongside the analysis (Re = 2.5 ± 1.1 pg and 0.10 ± 0.05 pg, respectively, with an $^{187}\text{Os}/^{188}\text{Os}$ of $0.25 \pm$
164 0.05 . The Re and Os uncertainties presented in Table 1 are determined by the full propagation of
165 uncertainties from the mass spectrometer measurements, blank abundances and isotopic compositions,
166 spike calibrations, and the results from analyses of Re and Os standards (running averages; Restd =
167 0.59782 ± 0.0005 ; DROs = 0.16083 ± 0.00005). The Re standard data together with the accepted
168 $^{185}\text{Re}/^{187}\text{Re}$ ratio (0.59738; Gramlich *et al.* 1973) are used to correct for mass fractionation.

169 *Sulphur isotope analytical methods*

170 Sulphur isotope analysis was performed on several milligrams of sulphide using the analytical protocol of
171 Robinson & Kusakabe (1975). Isotope ratios were measured on a VG SIRA II dual inlet mass spectrometer
172 and the data are reported in the conventional delta per mil notation relative to standard V-CDT ($\delta^{34}\text{S}$ ‰
173 V-CDT). Analytical precision at one sigma is $\pm 0.2\text{‰}$ for isotopically homogeneous material; for
174 standardisation NBS 123 gives -17.1‰ and IAEA S-3 gives -32.1‰ .

175

176 **Field and cross-cutting relationships, Loch Assynt shore**

177 *Early basement features*

178 Low-lying outcrops of Lewisian gneisses occur on the NE coast of Loch Assynt and immediately SW of the
179 A838 Inchnadamph-Lochinver road (Figs 2a, b; map reference NC 21 25). These easily accessible exposures
180 have been visited by generations of UK geology students during university-run field trips and are widely
181 referred to in published field guides (e.g. Johnson & Parsons 1979; Smith & Raine 2011). The amphibolite-
182 to granulite-facies TTG gneisses of the Assynt Terrane here show foliation and compositional banding
183 development (e.g. Fig. 3a) from millimetre to tens of metre scales (e.g. Sheraton *et al.* 1973). The foliation
184 is best developed in intermediate composition gneisses, where it is defined by 0.5–5 cm thick layers of
185 contrasting light (plagioclase and quartz) and dark (pyroxene, hornblende and biotite) layers, with
186 individual layers rarely continuing laterally for more than a few metres (Jensen 1984). Ultramafic units
187 typically occur as lensoid pods up to several tens of cm across, flattened in and wrapped by the foliation.
188 Representative samples from the intermediate composition gneisses in the Loch Assynt area typically
189 contain 30% quartz, 20% plagioclase, 10% microcline, 10% orthopyroxene and 30% heavily retrogressed
190 clinopyroxene. The mafic minerals are typically partially to wholly replaced by fine grained intergrown
191 aggregates of hornblende, actinolite, epidote and chlorite (Vernon *et al.* 2014). Foliations in the gneisses
192 dip moderately to the WNW (Fig 2ci), with isolated, cm-scale open to tight minor folds preserved locally.

193 Mineral lineations defined by aligned mafic minerals and elongate quartz-feldspar aggregates plunge NW
194 down the dip of the associated foliation and sub-parallel to minor fold hinges (Fig 2ci). Structures of this
195 kind and orientation are typical of c. 2.7-2.8 Ga Badcallian structures in the Assynt Terrane (Sheraton *et*
196 *al.* 1973), an inference confirmed by the fact that they are all cross cut by the Scourie dykes (see below).
197 There is no evidence in the area shown in Figure 2a for the development of the NW-SE Inverian structures
198 seen in other parts of the Assynt Terrane.

199 The fabrics in the gneisses are cross-cut at high angles by two steeply-dipping to sub-vertical NW-SE
200 dykes assigned to the c. 2.0-2.4 Ga Scourie dyke suite (Fig. 2a; Johnson & Parsons 1979). A c. 9 m thick
201 fine to medium grained ultramafic dyke, which lies to the SW, is only exposed in shoreline exposures at
202 [NC2124 2504]. It displays a chilled northern contact with the gneisses (the southern contact is not seen)
203 and has been described as a feldspathic picrite (Johnson & Parsons 1979). The c. 45 m wide sub-parallel
204 dyke located a few metres to the N is much better exposed both along the shoreline and inland, with
205 discordant igneous contacts exposed at a number of locations (e.g. Fig. 3b; NC 2105 2519, 2114 2519 and
206 2147 2503). This dyke too displays a well-developed chilled margin up to 0.5m thick and, where least
207 deformed, preserves relict igneous textures. However, olivine, orthopyroxene and clinopyroxene are
208 largely replaced by blue green hornblende which occurs in addition to calcic plagioclase and minor quartz
209 and ore.

210 The dykes – and older foliations in the gneisses - are both cross-cut by clusters of mainly NE-SW-
211 trending sub-vertical quartz-pyrite veins individually up to 0.5 m thick (Figs 2cii, 3c) and dated at c. 2.25
212 Ga by Vernon *et al.* (2014) using Re-Os geochronometry. Vein margins locally preserve evidence for syn-
213 emplacement sinistral shearing based on the local preservation of sub-horizontal quartz slickenlines, en
214 echelon offshoot veins and dilational jogs (Vernon *et al.* 2014).

215 Elsewhere in the Assynt Terrane, the quartz-pyrite veins and dykes are consistently overprinted and
216 reworked by lower amphibolite to upper greenschist facies dextral shear fabrics related to the Laxfordian
217 event, including the development of the central part of the Canisp Shear Zone (Fig. 1b; Attfield 1987). No
218 field evidence for such ductile dextral fabrics is preserved in the Loch Assynt exposures and the c. 2.25 Ga
219 quartz pyrite veins here are notably little deformed and show no significant grain-scale deformation
220 textures at temperatures greater than 300°C (Vernon *et al.* 2014).

221 *Brittle structures*

222 All of the features described in the preceding section are cross-cut by brittle faults, associated cataclastic
223 fault rocks and, locally, mineralization. These fall into two groups: one which pre-dates and a second which
224 post-dates deposition of the Torridonian and Cambro-Ordovician cover sequences. The dominant set in
225 the earlier group are NW-SE trending faults which are mostly sub-vertical to steeply NE dipping (Fig. 2ciii).
226 These comprise either clean break faults lined with narrow (<5 mm wide) seams of epidote-mineralized
227 cataclasite (Fig. 3d) or en-echelon arrays of ESE-WNW-trending tensile veins (<5 mm wide) filled with fine
228 epidote and quartz (Figs 2cv, 3e, f). Slickenline and quartz-epidote slickenfibres lineations on exposed fault
229 surfaces are moderately to shallowly dipping and associated brittle shear criteria everywhere indicate
230 sinistral senses of shear; local offsets of up to 0.5m are observed locally (e.g. Fig. 3d). These structures are
231 found in most exposures and lie sub-parallel to the sinistral Loch Assynt Fault which lies no more than a
232 few hundred metres to the SW (Fig. 1c; Krabbendam & Leslie 2010).

233 Another set of very much subordinate, sub-vertical to steeply N dipping fractures trend E-W (Fig.
234 2civ) and is associated with the same quartz-epidote mineralization. Moderately plunging slickenlines are
235 locally preserved in exposed fault surfaces, with offset markers and en-echelon arrays of quartz-epidote-
236 filled, WNW-ESE tensile fractures (Fig. 2cv) indicating dextral senses of shear. In a few localities, these

237 structures occur in conjugate arrays with NW-SE sinistral faults which share the same fills (Fig. 3f). They
238 are thus thought to be contemporaneous with, and antithetic to the dominant NW-SE sinistral faults.

239 The later set of faults are high angle normal faults with generally dip-slip slickenline lineations (Fig.
240 2cvi) and local developments of incohesive fault gouge and calcite mineralization (Pless 2012). Map scale
241 faults are NE-SW and NW-SE trending with displacements of up to several tens of metres based on offsets
242 of cover sequence boundaries (Fig. 2a). These normal faults are thought to be Mesozoic based on the
243 preservation of relatively incohesive gouges consistent with formation close to the surface, the
244 development of associated calcite mineralization and their regional relationship to outliers of Permian
245 and younger strata elsewhere in NW Scotland (Wilson *et al.* 2010; Krabbendam & Leslie 2010; Pless 2012).

246 A localised irregular region of copper mineralisation measuring $\sim 3 \times 3.5$ cm occurs on one of the
247 small islands close to the N shore of Loch Assynt (NC 2127 2497). Here bright-green and dark metallic grey
248 minerals occur within a dilational jog located close to intersection between an E-W fault (089/83N) and
249 slightly more NE trending quartz vein belonging to the c. 2.25 Ga set (Fig. 4a-c). En-echelon sets of WNW-
250 ESE tensile fractures (118/68NNE) associated with the fault suggest a dextral sense of shear consistent
251 with the subordinate set of early pre-Torridonian antithetic structures described above.

252 In addition to samples taken for geochemical and geochronological purposes, an oriented polished
253 thin section was made showing the local setting of the mineralization and how it cross-cuts both the
254 gneisses and the quartz vein seen in the field; it also includes a marginal part of the dextral E-W fault (Fig.
255 4c). This thin section was then studied using optical (transmitted and reflected light) microscopy and an
256 SEM, supplemented by an XRD analysis of a crushed sub-sample of the mineralization from the same
257 specimen.

258 **Petrography and mineralogy**

259 *Host rock and quartz vein*

260 The Lewisian wall rocks comprise medium to coarse grained sericitized calcic plagioclase (80% of rock),
261 biotite, chlorite and ore (after hornblende?), epidote and minor quartz with a weak foliation defined by
262 compositional banding and alignment of mineral grains (Fig 4c). The quartz vein is very coarse grained (up
263 to 15mm diameter grains) with local recrystallization and subgrain development consistent with a weak
264 low temperature deformational overprint (see Vernon *et al.* 2014 for descriptions of similar textures in
265 this region of Assynt). Brittle fractures and microcracks are widespread, but there is little evidence for
266 significant cataclasis other than in shears close to the E-W dextral fault (see below).

267 *Mineralized area*

268 An XRD and thin section analysis of the mineralized material reveals a complex array of copper sulphides
269 (anilite, djurleite; ca. 40% intergrown in roughly equal amounts), copper iron sulphide (bornite, ca. 30%),
270 iron oxide (hematite, ca. 20%) and sulphate (barite, ca. 10%) (Fig. 5a). The latter mineral is found only in
271 the mineralized area, most notably in its centre (Fig. 5b, c).

272 Reflected light optical microscopy of the main area of sulphide mineralization, most of which is
273 opaque in transmitted light, reveals complex fine intergrowths of anilite, djurleite, bornite, barite and
274 hematite (Figs 6a-c). Regions with hematite (some in discontinuous veinlets) and barite present are
275 commonly poor in intergrown bornite (e.g. Fig. 6b) suggesting that all these minerals are co-genetic.
276 Supergene alteration of <10% of copper sulphides to covellite and malachite is seen round many grain
277 boundaries, along cleavage planes and in locally developed cracks (Fig. 6c). Contacts between the copper-
278 iron mineralization and both the host quartz vein and the barite are characterized by bornite-poor rims
279 +/- hematite intergrowths (Fig. 6d). Sulphide-quartz boundaries are sharp with local alteration to fibrous
280 malachite (green), azurite (blue) and chlorite. Sulphide-gneiss contacts are more complex. Host rock
281 feldspars are altered to epidote, which is intergrown with fine hematite, bornite and copper sulphide (Figs

282 6e, f). The mineralization develops rimmed textures which show cusped-lobate forms consistent with the
283 operation of diffusion mechanisms during mineral growth (Passchier & Trouw 2005).

284 *Brittle-viscous shears*

285 Zones of shearing are mostly located along the margins of the thin section close to the E-W dextral fault
286 seen in the field (Fig. 4c), but poorly developed sub-parallel displacement zones occur as anastomosing
287 arrays elsewhere in the gneisses. Away from the region of copper mineralization, the shears are associated
288 with the deformation and new growth of iron oxides and chlorite which form asymmetric fibrous
289 overgrowths consistent with the operation of low temperature diffusive mass transfer mechanisms
290 synchronous with dextral shearing (Fig. 7a). The dextral shears also cut through the copper mineralization
291 and appear to smear it along the fault planes when viewed with the naked eye (e.g. Fig. 4c). In reflected
292 light and SEM images, the shears are seen to be associated with the new growth of fibrous copper
293 sulphides (often partially altered to malachite), chlorite, barite, hematite and epidote with an asymmetric
294 form consistent with the dextral shear sense (Figs 7b, c). This suggests that mineral growth and shearing
295 overlap and are associated with the operation of diffusive mass transfer processes along fluid-rich fault
296 zones. Shears closest to the mesoscale dextral fractures on the edge of the sample additionally host
297 spectacular zoned colloform intergrowths of malachite, libethenite (copper phosphate) and brochantite
298 (copper sulphate) (Fig. 7d), all formed by presumably somewhat later low temperature fluid flow along
299 open fractures. These late phases cross-cut and therefore locally post-date the fibrous minerals seen in
300 the shears, but are responsible for the bright green and blue colours seen in outcrop.

301 In summary, the XRD, petrological and microstructural observations suggest that the growth of
302 the copper-iron sulphide and associated mineralization at least overlaps in time with dextral shearing
303 along this E-W Late Laxfordian fault. This syn-tectonic relationship is based primarily on the observed
304 growth of fibrous sulphides along dextral shears spatially associated with a mesoscale fault seen in the

305 field (Figs 7b,c). The widespread growth of epidote co-genetically with sulphide mineralization (e.g. Figs
306 6e-f) also fits this interpretation as this mineral is very widely associated with so called 'Late Laxfordian'
307 structures both locally (e.g. Figs 3e-f) and regionally (Beacom *et al.* 2001). Thus it is argued that
308 geochronological dating of the sulphide mineralization also gives an age for the pre-Torrisonian brittle
309 faulting event in this part of the Assynt Terrane. Note that we believe that the analysis of a single bulk
310 sample of copper mineralization is justified by the textural observations which show that all the sulphides
311 are co-genetic (e.g. Figs 6a, b, d).

312

313 **Rhenium-osmium geochronology**

314 The analysed copper sulphide separate contains a total Re and Os abundance of 10 ppb and 179 ppt,
315 respectively (Table I). The elevated $^{187}\text{Re}/^{188}\text{Os}$ (3700) and $^{187}\text{Os}/^{188}\text{Os}$ (97) values indicate that the bulk of
316 the Os budget in the sample is radiogenic ^{187}Os ($^{187}\text{Os}^r$). To calculate a model Re-Os date the abundance
317 of $^{187}\text{Os}^r$ must be obtained. Given that we only have one sample due to the fact copper mineralization is
318 restricted to only a small area (3 x 3.5 cms), the $^{187}\text{Os}^r$ can only be determined using an assumed initial
319 $^{187}\text{Os}/^{188}\text{Os}$ composition, rather than a composition determined from the regression of Re-Os data of
320 several contemporaneous samples (e.g. Vernon *et al.* 2014). Using a moderately non-radiogenic
321 $^{187}\text{Os}/^{188}\text{Os}$ value of 0.2 ± 0.1 , 99.8 % of the ^{187}Os is radiogenic (Table I); coupled with the ^{187}Re data, a Re-
322 Os model date of 1555.3 ± 17.1 Ma is obtained using the ^{187}Re decay constant of $1.666 \times 10^{-11}\text{a}^{-1}$ (Smoliar
323 *et al.* 1996). However, given that fluid flow associated with the quartz veining and copper mineralization
324 is through c. 2.7 and 2.4 Ga crustal units of the Assynt Terrane, the fluid $^{187}\text{Os}/^{188}\text{Os}$ value could have been
325 significantly more radiogenic, although sulphur isotope analysis suggests that the sulphur associated with
326 the copper mineralization and 2.2 Ga pyrite is isotopically indistinguishable from primitive mantle (this
327 study – see below; Vernon *et al.* 2014). Although exhibiting large uncertainties, the initial $^{187}\text{Os}/^{188}\text{Os}$ for
328 2.2 Ga pyrite were shown to be 0.9 ± 9 and 3 ± 13 (Vernon *et al.* 2014). A more radiogenic initial $^{187}\text{Os}/^{188}\text{Os}$

329 results in the percentage of the ^{187}Os budget being slightly less radiogenic. For an initial $^{187}\text{Os}/^{188}\text{Os}$ of 0.9,
330 99.1 % of the ^{187}Os is radiogenic and 96.7 % for an initial $^{187}\text{Os}/^{188}\text{Os}$ of 3. Regardless of the value of the
331 initial $^{187}\text{Os}/^{188}\text{Os}$, the majority of the ^{187}Os budget (> 96 %) is radiogenic. As a result, the Re-Os model
332 dates are very similar (1555.3 [initial $^{187}\text{Os}/^{188}\text{Os}$ of 0.2] vs 1544.2 [initial $^{187}\text{Os}/^{188}\text{Os}$ of 0.9] vs 1511 [initial
333 $^{187}\text{Os}/^{188}\text{Os}$ of 3]; Table I). We therefore consider the copper mineralisation and by inference the
334 precipitation of the associated quartz vein(s) and fracture formation to have occurred at c. 1.55 Ga (Fig.
335 8a).

336 Sulphur isotope analysis

337 In their analysis of the earlier suite of c. 2.25 Ga quartz-pyrite veins in the Assynt Terrane, Vernon *et al.*
338 (2014) obtained one rather imprecise and significantly different age of c. 1.6 Ga from a pyrite sample at
339 the Waterworks locality in the CSZ near Lochinver (Fig. 1b). The five sulphides showing 2.25 Ga ages had
340 $\delta^{34}\text{S}$ (V-CDT) in the range 3.0 to 0.9 ‰ (averaging 1.7 ± 0.8 ‰, 1σ , $n=5$) whereas the sample from
341 Waterworks giving the 1.6 Ga age had $\delta^{34}\text{S}$ of -2.2 ‰, leading Vernon *et al.* (2014) to speculate that it
342 could represent a younger mineralization event. This age lies well within uncertainty of the Loch Assynt
343 analysis obtained here for which sulphide $\delta^{34}\text{S}$ is 0.0 ‰. There are several points worthy of note here.
344 Firstly, Lowry *et al.* (2005) in their compilation of sulphur isotope data and mineralogy of ore deposits in
345 northern Britain note that data from Lewisianoid basement inliers interleaved with the Moine Supergroup
346 cover sequences suggest "...a source of slightly ^{34}S -enriched sulphur in the range -3 ‰ to +5 ‰",
347 consistent with the vein data discussed above and an original mantle source for the sulphur as concluded
348 by Vernon *et al.* (2014). Secondly, the observation in this study of likely co-genetic ore sulphides and
349 barite, and the accompanying stable isotope partitioning (perhaps assuming isotopic as well as textural
350 equilibrium) between reduced and oxidised sulphur render further interpretation to the attribution of a

351 definitive fluid $\delta^{34}\text{S}$ unwise without a much more detailed study of the distribution of sulphur isotopes
352 amongst co-existing mineral phases (and an estimate of fluid pH and $f\text{O}_2$).

353 **Discussion**

354 *The age and regional extent of the 'Late Laxfordian' event*

355 The so-called 'Late Laxfordian' event is widely recognised in the Assynt Terrane and is associated with the
356 development of steeply-dipping to sub-vertical, NW-SE sinistral fault zones which commonly, but not
357 exclusively, reactivate similarly oriented Scourie dyke margins and Inverian-Laxfordian shear zone fabrics
358 (Attfield 1987; Beacom *et al.* 2001, Wilson *et al.* 2011). Epidote mineralized cataclasites and local
359 developments of pseudotachylite are also associated with these structures (Beacom 1999; Hardman
360 2019). The regional-scale Loch Assynt Fault is thought to have initiated as one of these structures
361 (Krabbendam & Leslie 2010) and is thought, at least in part, to reactivate the earlier Stoer Shear Zone
362 seen at the NW end of Loch Assynt (Fig. 1b). The fault can be traced 15 km northwestwards to a coastal
363 gully near Clashnessie (NC 0678 3169). Here it is associated with the development of a highly cemented
364 hematite stained breccia zone ~10 m wide with sub-horizontal slickenlines on exposed slip surfaces and
365 quartz-chlorite-epidote veins (Scott 2018). This fault does not cut – and therefore likely pre-dates – the
366 basal unconformity of the ca 1200 Ma Stoer Group which lies along strike and to the northwest (Fig. 1b).
367 In the region of Loch Assynt, the southeastern end of the fault has clearly experienced later reactivation
368 as it offsets the foreland sedimentary sequences (Torridon Group, Cambro-Ordovician marine sequences)
369 by 1300 m sinistrally and 120 m vertically (SW-side up) and also continues up into the lower parts of the
370 overlying Moine Thrust Zone (see Krabbendam & Leslie 2010). A related fault with the same trend and
371 smaller amounts of apparently sinistral and/or SW-side-up senses of offset is also seen displacing and
372 locally folding the basal Cambrian sequence north of the A837 Inchnadamph-Lochinver road (Fig. 2a; folds
373 seen 250 m NW of Lochan Feoir at NC 226 254).

374 We have shown that the *c.* 1.55 Ga copper-iron sulphide mineralization seen on the shore of Loch
375 Assynt is related to dextral E-W faulting that is antithetic to the more widespread NW-SE sinistral faults
376 seen in the area. We propose that these are typical 'Late Laxfordian' structures based on geometric and
377 kinematic similarity with other structures assigned to this group elsewhere in the Assynt Terrane (Fig. 8a;
378 e.g. Beacom 1999, Beacom *et al.* 2001; Wilson *et al.* 2011) and the widespread development of associated
379 epidote mineralization along these faults. Additional support for relating the brittle structures seen on
380 the north shore of Loch Assynt with regional brittle strike-slip faults comes from the local preservation of
381 low temperature ultramylonites and pseudotachylytes along the reactivated NW-SE margins of the larger
382 Scourie dyke in both gneiss (NC 21045 25192) and dyke (NC 21489 25025) (e.g. Figs 8b – d; Scott 2018).
383 The ultramylonites here are characterised by pervasive sub-grain rotation recrystallization with sinistral
384 S-C fabrics, minor folds and sigma porphyroclasts of both plagioclase and epidote (Fig. 8b). Quartz epidote
385 veins run sub-parallel and at high angles to the foliation, with the former being frequently partially
386 mylonitized or fibrous in form suggesting that mineralization occurred prior to, during and after local
387 crystal plasticity. Discrete microscale faults also offset marker layers sinistrally, with associated dextral
388 antithetic faults, and both root upwards and downwards into foliation-parallel detachments, some of
389 which follow the deformed quartz-epidote layers (Figs 8b-d). These detachment faults are lined by dark
390 brown pseudotachylytes, which locally show 'paired generation zone' (Grocott, 1981) geometries (Fig.
391 8d). Pseudotachylytes also form small (50 μm wide, ≤ 1 mm long) en-echelon injection veins once again
392 consistent with sinistral shear (e.g. Figs 8b-d). These fault rock assemblages are typical of 'Late Laxfordian'
393 faults in other regions (Beacom 1999; Beacom *et al.* 2001; Shihe & Park 1993).

394 In their analysis of the *c.* 2.25 Ga quartz-pyrite veins of the Assynt Terrane, one sample from the
395 Waterworks locality in the CSZ near Lochinver (Fig. 1b) yielded, although imprecise (± 1.3 Ga), a
396 significantly different age of *c.* 1.6 Ga (Vernon *et al.* 2014). The uncertainty in the presented Re-Os model
397 date of the sample is largely controlled by the uncertainty in the initial $^{187}\text{Os}/^{188}\text{Os}$ used to calculate $^{187}\text{Os}^f$

398 obtained from the regression of the Re-Os data (0.9 ± 9 ; Vernon et al. 2014). If a nominal uncertainty of
399 0.1 in the initial $^{187}\text{Os}/^{188}\text{Os}$ is used, the uncertainty in the Re-Os model date reduces significantly to 0.2
400 Ga. Additionally, the Waterworks pyrite sample also exhibits a lower sulphur isotope signature compared
401 to the other c. 2.25 Ga pyrite samples, which led Vernon et al. (2014) to speculate that it could represent
402 a younger mineralization event. Interestingly, the Re-Os model age of the Waterworks pyrite sample is
403 similar within uncertainty to that of the copper mineralization of Loch Assynt obtained here. Although
404 there are only two samples, regression of the $^{187}\text{Re}/^{188}\text{Os}$ vs $^{187}\text{Os}/^{188}\text{Os}$ data for the Waterworks sample
405 and the copper mineralization of this study yield a Re-Os date of 1538 ± 34 Ma, with an initial $^{187}\text{Os}/^{188}\text{Os}$
406 of 1.3 ± 1.8 . This potentially suggests a more regional deformation-hydrothermal event across the Assynt
407 Terrane at c. 1.55 Ga (Fig. 8a).

408 Superficially similar NW-SE sinistral faults associated with so called 'Late Crush Belts' are also
409 recognised in the Gairloch region which forms part of the Gruinard Terrane lying immediately to the SW
410 of the Assynt Terrane (Fig. 1a; Campbell *et al.* 2019). These zones are associated with extensive
411 developments of cataclasite and pseudotachylyte and were assigned to the same suite of 'Late Laxfordian'
412 structures in the regional studies of Beacom (1999) and Beacom *et al.* (2001).

413 Sherlock *et al.* (2008) used infrared laserprobe $^{40}\text{Ar}/^{39}\text{Ar}$ dating to date pseudotachylyte and host-
414 rock minerals at Gairloch. Complex results were attributed to the presence of refractory host-rock clasts
415 and mineral fragments in the pseudotachylyte and, on removing these complexities, the authors proposed
416 ages for the friction melts of between 0.98 and 1.12 Ga, i.e. Grenvillian. Interestingly, these authors also
417 obtained $^{40}\text{Ar}/^{39}\text{Ar}$ ages of 1.69-1.56 Ga from hornblende grains in the immediate host rocks adjacent to
418 pseudotachylyte-bearing crush zones, whereas biotites yielded ages of 1.30 - 1.03 Ga, suggestive of a later
419 tectonic event that did not exceed the closure temperature of Ar within the amphiboles ($\sim 500^\circ\text{C}$). They
420 attributed the older country rock ages to Laxfordian regional metamorphism and cooling, but they also lie
421 close to the c. 1.55 Ga age obtained during the present study. Host rock mineral ages can also be related

422 to local frictional melting events (e.g. Kelley *et al.* 1994) and it is clear that the crush zones at Gairloch
423 show widespread local evidence for multiple movement and melting episodes along individual slip zones
424 (Shihe & Park 1993; Beacom 1999; Campbell *et al.* 2019). Hence, we tentatively suggest that the older
425 ages at Gairloch are related to frictional heating during the *initiation* of the NW-SE crush belts in Gairloch
426 and that these structures were then reactivated during the Grenvillian as proposed by Sherlock *et al.*
427 (2008). Thus we suggest that the *c.* 1.55 Ga age obtained using Re-Os geochronology at Loch Assynt
428 plausibly gives an age for the regional *initiation* of 'Late Laxfordian' structures across both the Assynt and
429 Gairloch terranes in NW Scotland.

430

431 *The 'Assyntian' event: a proposal*

432 The foregoing discussion highlights the likelihood that the *c.* 1.55 Ga shearing event is of regional extent
433 through a large proportion of the Lewisian Complex, as suggested by Beacom *et al.* (2001). A palaeostress
434 inversion was undertaken using inferred opening directions from tensile veins and slip vectors taken from
435 measured shear fracture slickenline lineations using the Right Dihedron Method of Angelier & Mechler
436 (1977) (Figs 9ai-iii). These yield broadly E-W horizontal compression and N-S horizontal extension
437 directions with principle stress axes consistent with a strike-slip tectonic environment (σ_2 vertical,
438 Fig. 9b). As bedding in the local *c.* 1040 Ma Torridon Group strata that unconformably overlie the Assynt
439 Lewisian basement is subhorizontal, we see no reason to re-orient the structural data or analysis. An
440 inversion analysis of the later cross-cutting normal fault sets (Fig. 9aiv) yields a very different E-W
441 extension and a principle stress pattern consistent with normal faulting (σ_1 vertical) of likely
442 Mesozoic age (Pless 2012; cf. Roberts & Holdsworth 1999).

443 The *c.* 1.55 Ga shearing event is kinematically distinct from the preceding Laxfordian ductile
444 deformation which is associated with *dextral* shear along regional and local NW-SE shear zones such as
445 the CSZ and Scourie dyke margins (Fig. 8a; Attfield 1987). In this regard, we believe that continued use of

446 the term 'Late Laxfordian' is misleading as it represents a kinematically distinct and later deformation
447 episode, albeit one much influenced by the presence of pre-existing dyke contacts and shear zones. In
448 terms of regionally recognised events seen in nearby continental regions, the c. 1.55 Ga age is broadly
449 contemporaneous with the latter stages of the Gothian orogeny in southern Scandinavia (Baltica),
450 associated with widespread crustal accretion and calc-alkaline volcanics (Gaál & Gorbatshev 1987,
451 Starmer 1996). It also lies within uncertainty of the close of the Labradorian Orogeny in Canada (Laurentia;
452 c. 1.71-1.62 Ga; Kamo *et al.* 1996, Rivers 1997) meaning that it is possible that the c. 1.55 Ga event
453 represents an important missing link in Scotland between these two regional episodes. In the light of this,
454 we tentatively propose here that the 'Late Laxfordian' event should be referred to in future as the
455 'Assyntian' in order to: a) separate it from the earlier Laxfordian events; and b) recognize its possible
456 regional development. Clearly much further work is needed to further constrain the age, extent and
457 regional significance of this brittle episode throughout the Lewisian Complex.

458

459 **Conclusions**

460 A distinctive set of steeply dipping sinistral and dextral brittle-viscous shears postdating local
461 Neoproterozoic Badcallian fabrics, Palaeoproterozoic Scourie dykes and quartz-pyrite veins are recognized
462 cutting Lewisian gneisses exposed on the northern shore of Loch Assynt, a well visited teaching locality in
463 the NW Scotland. A dominant set of NW-SE sinistral faults are parallel to the adjacent Loch Assynt Fault
464 and reactivate dyke margins leading to the local development of low temperature ultramylonites and
465 pseudotachylytes, whilst an E-W dextral set are subordinate and antithetic structures (Fig. 9c). Both fault
466 sets are closely associated with steeply dipping NW-SE tensile quartz-epidote filled tensile fractures/veins.
467 The association of these fault rocks with epidote-quartz-chlorite mineralization is typical of so-called 'Late
468 Laxfordian' events in the Assynt Terrane and beyond. One of the dextral E-W faults close to Loch Assynt
469 is associated the co-genetic development of copper-iron sulphides, iron oxide, epidote and barite.

470 Texturally, the mineralization is, at least in part, syn-tectonic based on the fibrous growth form of the
471 sulphide and oxide minerals grown along local dextral shears. A Re-Os age from the copper-iron sulphides
472 of c. 1.55 Ga likely dates the age of brittle shearing event in this terrane. Given its potential regional extent
473 we propose that this event should be referred to as the 'Assyntian' in order to distinguish it from earlier,
474 kinematically distinct Laxfordian events. The palaeocontinental significance of this strike-slip deformation
475 episode remains unproven, but overlaps in age with the closing stages of the Gothian and Labradorian
476 orogenies in Baltica and Laurentia, respectively, and may provide a structural link between these two
477 contemporaneous tectonic episodes located either side of Scotland in the Mesoproterozoic (e.g. see
478 Starmer 1996). The findings further illustrate the ability of the Re-Os geochronometer to date Proterozoic
479 sulphide deposits and associated deformation events.

480 **Acknowledgements**

481 We thank Durham University for supporting undergraduate field trips to the Assynt region over many years
482 and Chris Rix at Inchnadamph Lodge for accommodation, patience and space for our wonderful field dogs,
483 Ava and Tagish. Chris Ottley and Geoff Nowell are thanks for laboratory support. DS acknowledges the Total
484 Endowment Fund and the CUG Wuhan Dida Scholarship. George Guice, Graham Leslie and John MacDonald
485 are warmly thanked for their detailed constructive comments.

486 **References**

- 487 Angelier, J. & Mechler, P. 1977. Sur une méthode graphique de recherche des contraintes principales
488 également utilisable en tectonique et en séismologie: la méthode des dièdres droits. *Bulletin Societe*
489 *géologique France*, **19**, 1309–1318.
- 490 Attfield, P., 1987. The structural history of the Canisp Shear Zone, In: Park, R.G. & Tarney, J. (eds), *Evolution*
491 *of the Lewisian and comparable Precambrian High Grade Terrains*. Special Publication of the Geological
492 Society, London, **27**, 165-174.
- 493 Beacom, L.E., 1999. *The Kinematic Evolution of Reactivated and Non-Reactivated Faults in Basement Rocks,*
494 *NW Scotland*, Queens University, Belfast, Unpublished PhD thesis.
- 495 Beacom, L.E., Holdsworth, R.E., McCaffrey, K.J.W. & Anderson, T.B., 2001. A quantitative study of the
496 influence of pre-existing compositional and fabric heterogeneities upon fracture-zone development during
497 basement reaction, In; Holdsworth, R.E., Strachan. R.A., Magloughlin, J.F. & Knipe, R.J, (eds). *The Nature and*
498 *Tectonic Significance of Fault Zone Weakening*, Special Publication of the Geological Society, London, **186**,
499 195-211. <https://doi.org/10.1144/GSL.SP.2001.186.01.12>

- 500 Boyd, A.J. & Crichton, J.M. 1960. Discovery of Copper Minerals in Lewisian Gneiss. *Geological Magazine*, **98**,
501 88. <https://doi.org/10.1017/S001675680000013>
- 502 Campbell, L.R., Phillips, R.J., Walcott, R.C. & Lloyd, G.E. 2019. Rupture geometries in anisotropic amphibolite
503 recorded by pseudotachylytes in the Gairloch Shear Zone, NW Scotland. *Scottish Journal of Geology*.
504 <https://doi.org/10.1144/sjg2019-003>
- 505 Chapman, H.J. 1979. 2390 Myr Rb-Sr whole rock age for the Scourie dykes of north-west Scotland. *Nature*
506 277, 642-3.
- 507 Corfu, F., Heaman, L. & Rogers, G. 1994. Polymetamorphic evolution of the Lewisian Complex, NW Scotland,
508 as recorded by U-Pb isotopic compositions of zircon, titanite and rutile, *Contributions to Mineralogy and*
509 *Petrology*, 117, 215–228. <https://doi.org/10.1007/bf00310864>
- 510 Coward, M.P. & Park, R.G., 1987. The role of mid-crustal shear zones in the Early Proterozoic evolution of
511 the Lewisian, In; Park, R.G. & Tarney, J. (eds), *Evolution of the Lewisian and Comparable Precambrian High*
512 *Grade Terrains*, Special Publication of the Geological Society, London, **27**, 127-138.
- 513 Davies, J.H.F.L. & Heaman, L.M., 2014. New U-Pb baddeleyite and zircon ages for the Scourie dyke swarm:
514 A long-lived large igneous province with implications for the Paleoproterozoic evolution of NW Scotland.
515 *Precambrian Research*, **249**, 180-198, <https://doi.org/10.1016/j.precamres.2014.05.007>
- 516 Dickinson, B.B. & Watson, J. 1976. Variations in crustal level and geothermal gradient during the evolution
517 of the Lewisian Complex of northwest Scotland. *Precambrian Research*, **3**, 365-374.
- 518 Droop, G.T.R., Fernandes, L.A.D. & Shaw, S., 1989. Laxfordian metamorphic conditions of the
519 Palaeoproterozoic Loch Maree Group, Lewisian Complex, NW Scotland, *Scottish Journal of Geology*, **35**, 31-
520 50.
- 521 Friend, C.R.L. & Kinny, P.D., 2001. A reappraisal of the Lewisian Gneiss Complex: geochronological evidence
522 for its tectonic assembly from disparate terranes in the Proterozoic, *Contribution to Mineralogy and*
523 *Petrology*, **142**, 198-218.
- 524 Gaál, G. & Gorbatshev, R. 1987. An outline of the Precambrian evolution of the Baltic Shield, *Precambrian*
525 *Research*, **35**, 15–52. [https://doi.org/10.1016/0301-9268\(87\)90044-1](https://doi.org/10.1016/0301-9268(87)90044-1)
- 526 Gramlich, J.W., Murphy, T.J., Garner, E.L. & Shields, W.R., 1973. Absolute isotopic abundance ratio and
527 atomic weight of a reference sample of rhenium, *Journal of Research of the National Bureau of Standards*,
528 **77A**, 691–698.
- 529 Goodenough, K., Crowley, Q., Krabbendam, M. & Parry, S. 2013. New U-Pb age constraints for the Laxford
530 Shear Zone, NW Scotland: Evidence for tectono-magmatic processes associated with the formation of a
531 Paleoproterozoic supercontinent, *Precambrian Research*, **233**, 1–19.
532 <https://doi.org/10.1016/j.precamres.2013.04.010>
- 533 Grocott, J. 1981 Fracture geometry of pseudotachylyte generation zones: a study of shear fractures formed
534 during seismic events, *Journal of Structural Geology*, **3**, 169–178. [https://doi.org/10.1016/0191-
535 8141\(81\)90012-2](https://doi.org/10.1016/0191-8141(81)90012-2)

536 Guice, G.L., McDonald, I., Hughes, H.S.R., MacDonald, J.M., Blenkinsop, T.G., Goodenough, K.M., Faithfull,
537 J.W. & Gooday, R.J. 2018. Re-evaluating ambiguous age relationships in Archean cratons: implications for
538 the origin of ultramafic-mafic complexes in the Lewisian Gneiss Complex, *Precambrian Research*, doi:
539 <https://doi.org/10.1016/j.precamres.2018.04.020>

540 Hamilton, P., Evensen, N., O’Nions, R. & Tarney, J. 1979. Sm—Nd systematics of Lewisian gneisses:
541 implications for the origin of granulites, *Nature*, **277**, 25-28. <https://doi.org/10.1038/277025a0>

542 Hardman, K. 2019. Cracking Canisp: Deep void evolution during ancient earthquakes. *Geoscientist*, **29** (1),
543 10-15. <https://doi.org/10.1144/geosci2019-003>

544 Heaman, L.M. & Tarney, J., 1989. U-Pb baddeleyite ages for the Scourie dyke swarm, Scotland: evidence for
545 two distinct intrusion events, *Nature*, **340**, 705-708.

546 Jensen, L.N., 1984. Quartz microfabric of the Laxfordian Canisp Shear Zone, NW Scotland, *Journal of*
547 *Structural Geology*, **6**, 293-302.

548 Johnson, M. R.W. & Parsons, I. 1979. Assynt District of Sutherland - Geological Excursion Guide. Edinburgh
549 Geological Society, 76pp.

550 Kamo, S.L., Wasteneys, H., Gower, C.F. & Krogh, T.E. 1996. U-Pb geochronology of Labradorian and later
551 events in the Grenville Province, eastern Labrador, *Precambrian Research*, **80**, 239-260.

552 Kelley, S.P., Reddy, S.M. & Maddock, R. 1994. Laser-probe ⁴⁰Ar/³⁹Ar investigation of a pseudotachylite and
553 its host rock from the Outer Isles thrust, Scotland. *Geology*, **22**, 443–446.

554 Kinny, P.D. & Friend, C.R.L., 1997. U-Pb isotopic evidence for the accretion of different crustal blocks to form
555 the Lewisian Complex of northwest Scotland. *Contributions to Mineralogy and Petrology*, **129**, 326–340.

556 Kinny, P.D., Friend, C.R.L. & Love, G.L., 2005. Proposal for a terrane-based nomenclature for the Lewisian
557 Gneiss Complex of NW Scotland, *Journal of the Geological Society*, **162**, 175-186.

558 Krabbendam, M. & Leslie, A. (2010) ‘Lateral variations and linkages in thrust geometry: the Traligill
559 transverse zone, Assynt Culmination, Moine thrust belt, NW Scotland’, In: Law, R. D., Butler, R. W. H.,
560 Holdsworth, R. E., Krabbendam, M. & Strachan, R. A. (eds) *Continental Tectonics and Mountain Building: The*
561 *Legacy of Peach and Horne*. Geological Society, London, Special Publications, **335**, 335–357.
562 <https://doi.org/10.1144/sp335.16>

563 Love, G.J.L, Kinny, P.D. & Friend, C.R.L., 2004. Timing of magmatism and metamorphism in the Gruinard Bay
564 area of the Lewisian Gneiss Complex: comparisons with the Assynt Terrane and implications for terrane
565 accretion, *Contributions to Mineralogy and Petrology*, **146**, 620-636.

566 Lowry, D., Boyce, A.J., Fallick, A.E., Stephens, W.E & Grassineau, N.V. 2005. Terrane and basement
567 discrimination in northern Britain using sulphur isotopes and mineralogy of ore deposits. In: I. McDonald,
568 A.J. Boyce, I.B. Butler, R.J. Herrington and D.A. Polya (eds) *Mineral Deposits and Earth Evolution*, Geological
569 Society, London, Special Publication **248**, 133-151.

570 MacDonald, J.M., Goodenough, K.M., Wheeler, J., Crowley, Q., Harley, S.L., Mariani, E. & Tatham, D. 2015.
571 Temperature–time evolution of the Assynt Terrane of the Lewisian Gneiss Complex of Northwest Scotland

572 from zircon U-Pb dating and Ti thermometry. *Precambrian Research*, **260**, 55–75.
573 <https://doi.org/10.1016/j.precamres.2015.01.009>

574 Mason, A.J. 2016. The Palaeoproterozoic anatomy of the Lewisian Complex, NW Scotland: evidence for two
575 'Laxfordian' tectonothermal cycles, *Journal of the Geological Society*, **173**, 153-169.
576 <https://doi.org/10.1144/jgs2015-026>

577 O'Hara, M.J. 1961 Petrology of the Scourie dyke, Sutherland (Plate XVIII) *Mineralogical Magazine and*
578 *Journal of the Mineralogical Society*, **32**, 848-865. <https://doi.org/10.1180/minmag.1961.032.254.02>

579 Park, R.G. 1994. Early Proterozoic tectonic overview of the northern British Isles and neighbouring terranes
580 in Laurentia and Baltica, *Precambrian Research*, **68**, 65-79.

581 Park, R.G. 2002. *The Lewisian Geology of Gairloch, NW Scotland*, Geological Society of London, Memoir, 26,
582 pp 88.

583 Park, R.G. 2005. The Lewisian terrane model: a review. *Scottish Journal of Geology*, **41**, 105-118.

584 Park, R.G. & Tarney, J. 1987. The Lewisian Complex: a typical Precambrian high-grade terrane?, In: Park, R.G.
585 & Tarney, J. (eds), *Evolution of the Lewisian and Comparable Precambrian High Grade Terranes*, Special
586 Publication of the Geological Society, London, **27**, 13-26.

587 Park, R.G., Cliff, R.A., Fettes, D.J. & Stewart, A.D. 1994. Precambrian rocks in northwest Scotland west of the
588 Moine Thrust: the Lewisian Complex and Torridonian, In: Gibbons, W. & Harris, A.L. (eds), *A Revised*
589 *Correlation of Precambrian Rocks in the British Isles*, Geological Society, London, Special Report, **22**, 6-22.

590 Passchier, C.W. & Trouw, R.A.J., 2005. *Micro-Tectonics*, Springer Berlin Heidelberg, New York.

591 Petit, J.P. 1987. Criteria for the sense of movement on fault surfaces in brittle rocks. *Journal of Structural*
592 *Geology*, 9, 597-608, [https://doi.org/10.1016/0191-8141\(87\)90145-3](https://doi.org/10.1016/0191-8141(87)90145-3)

593 Pless, J. 2012. *Characterising fractured basement using the Lewisian Gneiss Complex, NW Scotland:*
594 *Implications for fracture systems in the Clair Field basement*. Unpublished PhD thesis, Durham University.

595 Rivers, T. 1997. Lithotectonic elements of the Grenville Province: review and tectonic implications.
596 *Precambrian Research*, **86**, 117-154, [doi.org/10.1016/S0301-9268\(97\)00038-7](https://doi.org/10.1016/S0301-9268(97)00038-7)

597 Roberts, A.M. & Holdsworth, R.E. 1999. Linking onshore and offshore structures: Mesozoic extension in the
598 Scottish Highlands. *Journal of the Geological Society, London*, **156**, 1061-1064.
599 <https://doi.org/10.1144/gsjgs.156.6.1061>

600 Robinson, B.W. & Kusakabe, M. 1975. Quantitative preparation of sulfur dioxide for 34S/32S analyses from
601 sulfides by combustion with cuprous oxide. *Analytical Chemistry*, **47**, 1179-1181.

602 Scott, L.J. 2018. *Dyke reactivation across the frictional-viscous transition: Precambrian deformation of*
603 *Scourie dyke margins in NW Scotland*. Unpublished MSc thesis, Durham University.

604 Selby, D., Kelley, K.D., Hitzman, M.W. & Zieg, J. 2009. Re-Os sulphide (Bornite, Chalcopyrite, and Pyrite)
605 systematic of the Carbonate-hosted copper deposits at Ruby Creek, Southern Brooks Range, Alaska,
606 *Economic Geology*, **104**, 437-444.

- 607 Sheraton, J.W., Tarney, J., Wheatley, T.J. & Wright, A.E. 1973. The structural history of the Assynt district,
608 In: Park, R.G. & Tarney, J. (eds), *The early Precambrian rocks of Scotland and related rocks of Greenland*,
609 Department of Geology, Keele, 31-44.
- 610 Sherlock, S.C., Jones, K.A. & Park, R.G. 2008. Grenville-age pseudotachylite in the Lewisian: laserprobe
611 $^{40}\text{Ar}/^{39}\text{Ar}$ ages from the Gairloch region of Scotland (UK), *Journal of the Geological Society*, **165**, 73-83,
612 <https://doi.org/10.1144/0016-76492006-134>
- 613 Shihe, L. & Park, R.G. 1993. Reversals of movement sense in Lewisian brittle–ductile shear zones at Gairloch,
614 NW Scotland, in the context of Laxfordian kinematic history, *Scottish Journal of Geology*, **29**, 9–19.
615 <https://doi.org/10.1144/sjg29010009>
- 616 Smith, M.P. & Raine, R. 2011. Excursion 1 – Loch Assynt and the Achmore duplex. In: Goodenough, K.M. &
617 Krabbendam, M. (eds): *A Geological Excursion Guide to the North West Highlands of Scotland*. Edinburgh
618 Geological Society, 37-52.
- 619 Smoliar, M.I., Walker, R.J., & Morgan, J.W. 1996. Re-Os isotope constraints on the age of Group IIA, IIIA, IVA,
620 and IVB iron meteorites, *Science*, **271**, 1099–1102.
- 621 Starmer, I.C. 1996. Accretion, rifting, rotation, and collision in the North Atlantic Supercontinent, 1700-950
622 Ma. In: Brewer, T., and Atkin, B. P. (eds.), *Precambrian crustal evolution in the North Atlantic regions*: Special
623 Publication of the Geological Society, London, **112**, 226-252.
- 624 Sutton, J. & Watson, J., 1950. The pre-Torridonian metamorphic history of the Loch Torridon and Scourie
625 areas in the north-west Highlands, and its bearing on the chronological classification of the Lewisian,
626 *Quarterly Journal of the Geological Society*, **106**, 241-307.
- 627 Tarney, J. 1973. The Scourie dyke suite and the nature of the Inverian event in Assynt, In: Park, R.G. & Tarney,
628 J. (eds), *The early Precambrian rocks of Scotland and related rocks of Greenland*, Department of Geology,
629 Keele, 105-118.
- 630 Vernon, R., Holdsworth, R.E., Selby, D., Dempsey, E., Finlay, A.J. & Fallick, A.E. 2014. Structural characteristics
631 and Re-Os dating of quartz-pyrite veins in the Lewisian Gneiss Complex, NW Scotland: evidence of an early
632 Palaeoproterozoic hydrothermal regime during terrane amalgamation. *Precambrian Research*, **246**, 256–
633 267, <https://doi.org/10.1016/j.precamres.2014.03.007>
- 634 Wheeler, J., Park, R.G., Rollinson, H.R. & Beach, A. 2010. The Lewisian Complex: insights into deep crustal
635 evolution, In: Law, R.D., Butler, R.W., Holdsworth, R.E., Krabbendam, M. & Strachan, R.A. (eds), *Continental*
636 *Tectonics and Mountain Buildings: The Legacy of Peach and Horne*, Geological Society, London, Special
637 Publications, **335**, 51-79. <https://doi.org/10.1144/SP335.4>
- 638 Wilson, R.W., Holdsworth, R.E., Wild, L.E., McCaffrey, K.J.W., England, R.W., Imber, J. & Strachan, R.A. 2010.
639 Basement-influenced rifting and basin development: a reappraisal of post-Caledonian faulting patterns in
640 the North Coast Transfer Zone, Scotland. In: Law, R.D., Butler, R.W.H., Holdsworth, R.E., Krabbendam, M. &
641 Strachan, R.A. (eds) *Continental Tectonics and Mountain Building: The Legacy of Peach and Horne*,
642 Geological Society, London, Special Publication, **335**, 795-826. <https://doi.org/10.1144/SP335.32>

643 Wilson, R.W., Holdsworth, R.E. & Wightman, R. 2011. Excursion 2 - Transect through the Canisp Shear Zone,
644 Achmelvich, North-west Highlands. In: Goodenough, K.M. & Krabbendam, M. (eds): *A Geological Excursion*
645 *Guide to the North West Highlands of Scotland*. Edinburgh Geological Society, 53-73.

646 Zhu, X. K., O'Nions, R. K., Belshaw, N. S. & Gibb, A. J., 1997. Lewisian crustal history from in situ SIMS mineral
647 chronometry and related metamorphic textures. *Chemical Geology*, **136**, 205-218.

648

649

650 **Figure Captions**

651 Figure 1) a) Regional location map with Lewisian Complex terranes in mainland of NW Scotland. Box shows
652 location of maps in b) and c). b) Simplified geological map of the Assynt Terrane with Inverian-Laxfordian
653 shear zones (in green) and trace of sub-vertical Loch Assynt Fault. Box shows location of Fig 2a. c) Simplified
654 regional map showing locations and NW-SE trend of Scourie dykes in the Assynt Terrane.

655 Figure 2) a) Simplified geological map of the N shore of central Loch Assynt (pink = Lewisian gneiss; green =
656 Scourie dykes; brown = Torridonian sandstones; orange = Cambrian Basal Quartzite; yellow = Cambrian Pipe
657 Rock Quartzite; heavy black lines are late normal faults). Contours in metres. Box shows location of Fig 2b.
658 b) GoogleEarth air photo of N shore showing location of mineralization (Fig. 4a). c) Equal area lower
659 hemisphere stereonet (i-vi) of structural data from the Lewisian Complex from the region shown in Fig 2a
660 and b.

661 Figure 3) Field outcrop relationships in Loch Assynt area. a) Typical banded dioritic-granodioritic gneisses
662 with WNW-dipping Badcallian foliation (NC 2110 2503). b) Plan view of NW-SE-trending northern contact of
663 thick Scourie dyke (dark rock, bottom) cross cutting foliation in Badcallian gneisses (top). Note interfingering
664 of dyke and gneiss (above and to the left of the compass clino) and local later brittle reactivation adjacent
665 to the original intrusive contact. (NC 2515 2518). c) Oblique view of undeformed NE-SW quartz-pyrite veins
666 (c. 2.25 Ga) cross-cutting Badcallian foliation in gneisses (NC 2117 2508). d) Oblique view of quartz-pyrite
667 veins offset by NW-SE subvertical sinistral fault; note pale green epidote mineralization to right of whistle
668 (NC 2110 2517). e) Plan view of NW-SE trending en-echelon array of tensile quartz-epidote veins cutting
669 gneisses (NC2124 2504). f) Plan view of conjugate sinistral and dextral en-echelon quartz-epidote tension
670 gashes – note sinistral offset of older quartz-pyrite vein (NC 2124 2504).

671 Figure 4) a) Drone-based plan view air photo of island where copper-iron mineralization occurs (yellow box)
672 with arrows showing NE-SW quartz-pyrite vein running across rock platform. b) Plan view of outcrop at
673 NC2127 2497 showing NE-SW quartz-pyrite vein (blue) cross-cut by copper iron mineralization (yellow) and

674 dextral faults (red). Location of thin section shown in Figure c also shown. c) Low power PPL view of thin
675 section showing contact relationships between gneisses, quartz-pyrite vein, copper-iron mineralization and
676 dextral faults.

677 Figure 5) a) XRD data of copper-iron mineralization sample from NC 2127 2497. b) low power and c) higher
678 power PPL thin section images of typical barite-ore intergrowth textures consistent with co-genetic mineral
679 growth.

680 Figure 6) Textural relationships consistent with cogenetic copper-iron-barite ore mineralization in thin
681 section. a) Reflected light image of fine intergrowths of anilite (pale yellow-green), djurleite (pale-medium
682 blue), bornite (pink), barite (grey) and hematite (yellow). Note that areas with intergrown hematite
683 generally lack intergrown bornite and vice versa. b) Reflected light image of discontinuous veinlet of
684 intergrown barite and hematite with bornite-free rim of anilite-djurleite. c) BSEM image of supergene
685 alteration of copper sulphides to covellite and malachite. Note dendritic growth forms and localization along
686 microcracks and cleavage planes. d) Reflected light image of intergrown copper sulphides and bornite
687 (bottom) adjacent to region of intergrown copper sulphides, hematite and barite which forms a contact
688 zone with larger region of barite (top). e) PPL transmitted and f) reflected light images of typical contact
689 zone between copper-iron mineralization (bottom) and feldspathic Lewisian gneiss (top). The feldspar is
690 altered to epidote and intergrown with fine hematite, bornite & Cu sulphide. The alteration rims show
691 cusate-lobate forms consistent with the operation of diffusion mechanisms during mineral growth.

692 Figure 7) Fibrous mineral growth textures associated with brittle-ductile dextral micros shears. a) PPL
693 transmitted light image of dextral asymmetric fibrous overgrowths of green chlorite and black hematite on
694 hematite porphyroclasts and along shear surfaces. b) BSEM and c) reflected light images of dextral
695 asymmetric fibrous growth of Cu sulphides (partly altered to malachite and sparse spots of bornite), epidote,
696 chlorite, barite & hematite. The fibrous zone cross cuts a more massive region of intergrown copper-iron
697 sulphides, hematite, barite and epidote. d) BSEM image of zoned colloform intergrowths of malachite,
698 libethenite (copper phosphate) and brochantite (copper sulphate) cross cutting fibrous copper sulphide and
699 chlorite seen in dextral shear.

700 Figure 8) a) Revised chronology of events and relation to regional assembly of the Lewisian Complex. b-d)
701 PPL transmitted light images of ultramylonite-pseudotachylyte and epidote-quartz mineralization in highly
702 deformed gneisses along Scourie dyke margin at NC 2104 2519. Note the widespread development of

703 sinistral shear criteria associated with both ultramylonite and pseudotachylyte development. Note also the
704 fibrous form of the epidote adjacent to some foliation-parallel shears.

705 Figure 9) a) Stress inversion data for i) sinistral faults; ii) dextral faults; iii) tensile fractures/veins; iv) later
706 (Mesozoic) normal faults. b) Stress inversion analysis for i) - iii) combined, with the Assynt Fault trend (red
707 dashed line) shown together with a summary of mean planes, shear senses and opening directions. c) 3D
708 summary diagram of fracture orientations and kinematics; not to scale.

709

710 **Table**

711 Table I) Re-Os and S isotope data for Copper mineral separate from vein in the Lewisian Complex, Loch
712 Assynt, NW Scotland.

713

714

Table 1: Re-Os and S isotope data for Copper mineral separate from a quartz vein in the Lewisian Complex, NW Scotland.

Batch/Sample	Location (Lat/Long)/OS	Re (ppb)	±	Os ¹ (ppt)	±	¹⁸⁷ Re (ppb)	±	¹⁸⁷ Os ² (ppt)	±	% ¹⁸⁷ Os ³	¹⁸⁷ Re/ ¹⁸⁸ Os	±	¹⁸⁷ Os/ ¹⁸⁸ Os	±	rho ³	Model age ⁴	±	Model age ⁵	±	Model age ⁶	±	δ ³⁴ S (per mil) ⁷
RO628-7_Cu sample		10.04	0.04	178.8	5.3	6.31	0.02	165.6	2.4	99.8	3699.7	80.8	97.3	2.3	0.889	1555.3	17.1	1544.2	17.1 [145.2]	1511	17.1 [209]	0.0

Notes (see text for details): All uncertainties are reported at the 2σ level. ¹⁸⁷Os/¹⁸⁸Os uncertainties reported at 2SE; all data are blank corrected, blanks for Re and Os were 2.4 ± 0.5 and 0.10 ± 0.05 pg, respectively, with an average ¹⁸⁷Os/¹⁸⁸Os value of 0.25 ± 0.05 (1SD, n = 1); All uncertainties are determined through the full propagation of uncertainties of the Re and Os mass spectrometer measurements, blank abundances and isotopic compositions, spike calibrations, and reproducibility of standard Re and Os isotopic values;

¹ Total Os abundance

² ¹⁸⁷Os² presented are calculated using an initial ¹⁸⁷Os/¹⁸⁸Os of 0.2 ± 0.1 (99.1% using an ¹⁸⁷Os/¹⁸⁸Os of 0.9, 96.7% using an ¹⁸⁷Os/¹⁸⁸Os of 3

³ rho is the error correlation

A model age can be directly calculated using $\ln(\text{Os}^{187}/\text{Re}) = \lambda t$

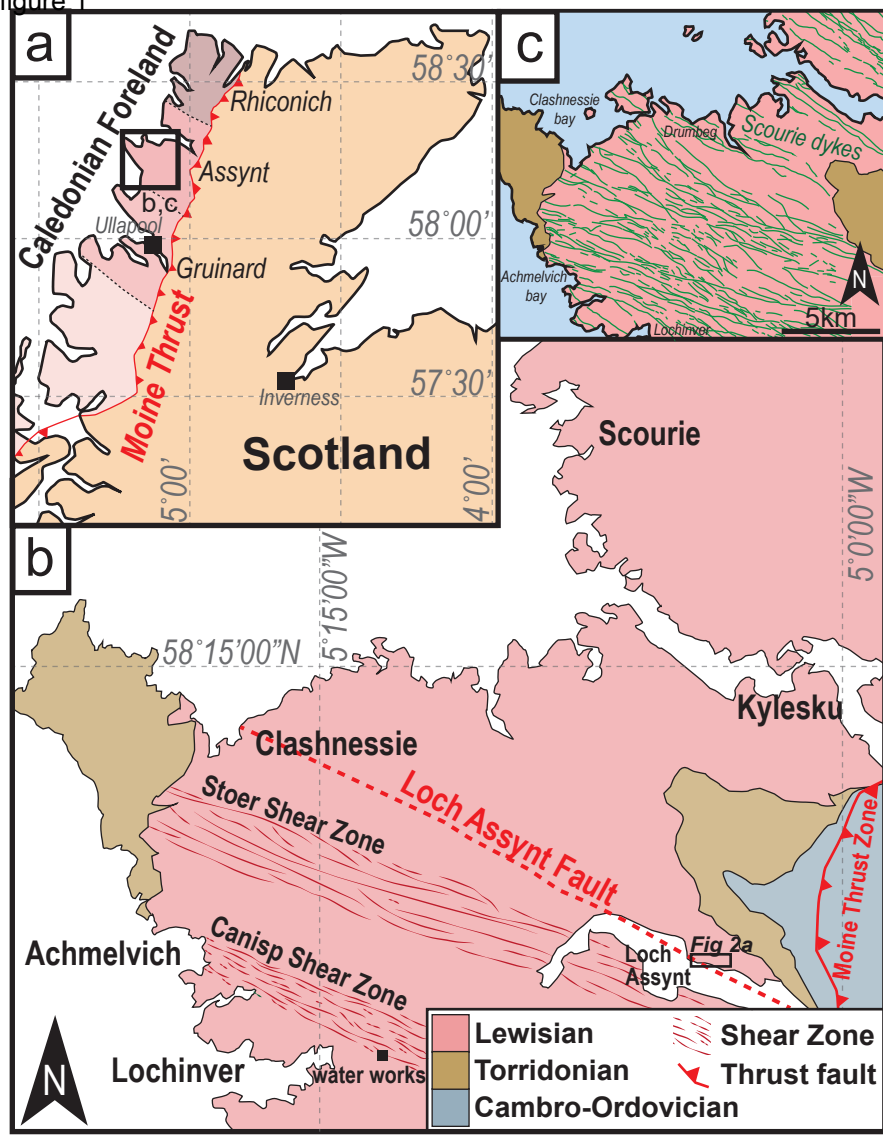
⁴ model age determined using an initial ¹⁸⁷Os/¹⁸⁸Os value of 0.2 ± 0.1

⁵ model age determined using an initial ¹⁸⁷Os/¹⁸⁸Os value of 0.9 ± 0.1 [9]. Bracketed value is the uncertainty from regression of the Re-Os data from Vernon et al. (2014).

⁶ model age determined using an initial ¹⁸⁷Os/¹⁸⁸Os value of 3 ± 0.1 [13]. Bracketed value is the uncertainty from regression of the Re-Os data from Vernon et al. (2014).

⁷ The reproducibility based on full replicate analyses of internal laboratory standards was ±0.2 per mil (1σ) VCDT

figure 1



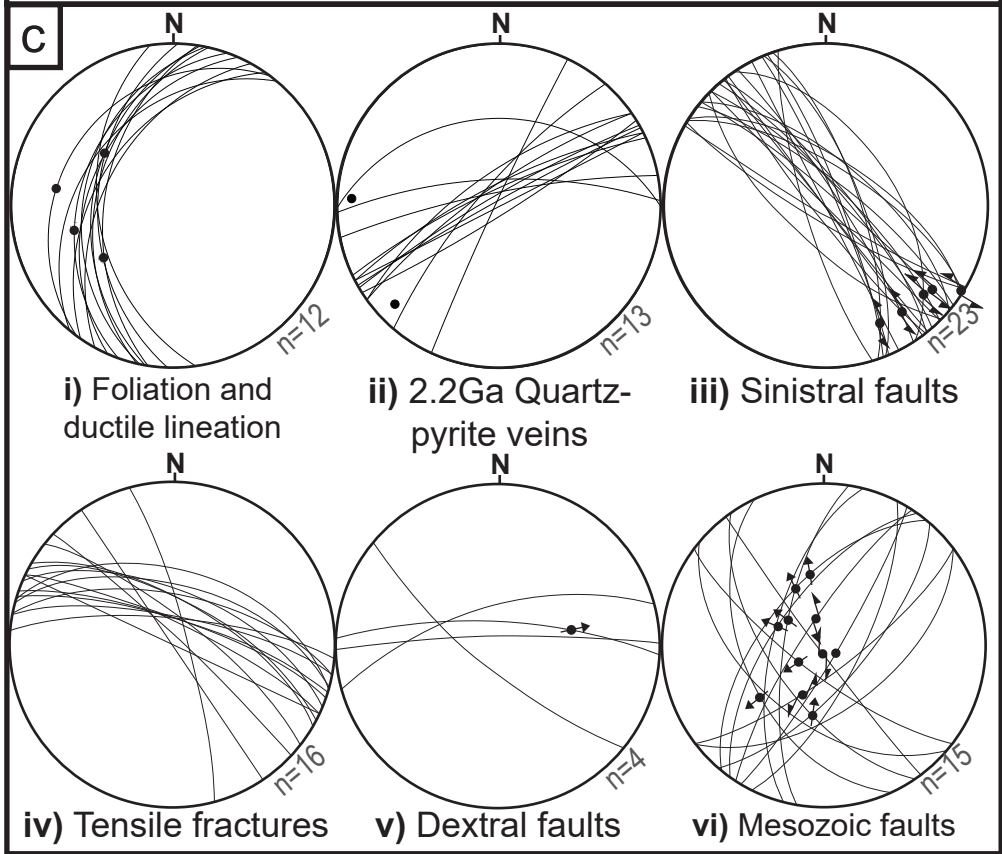
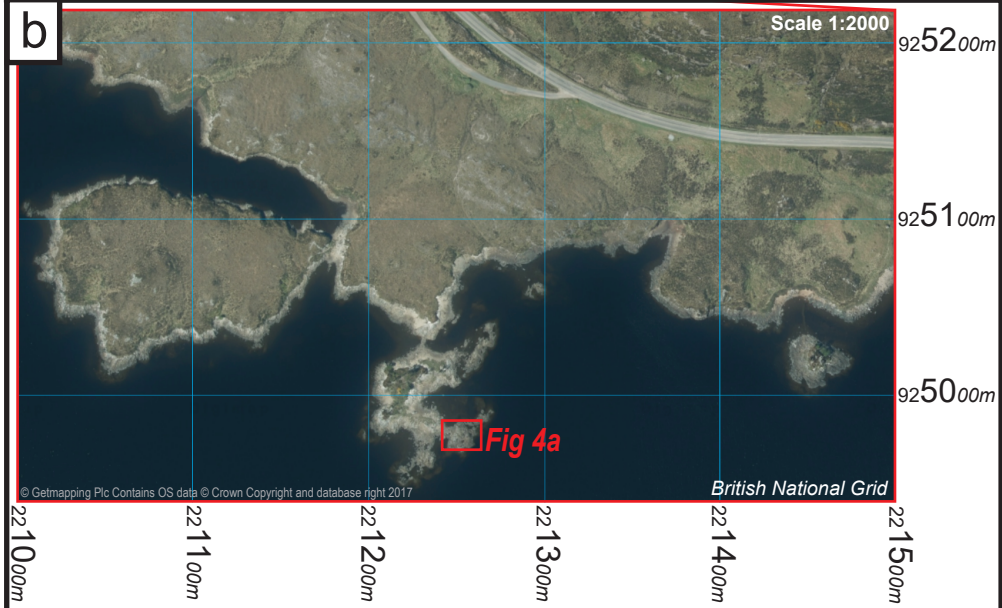
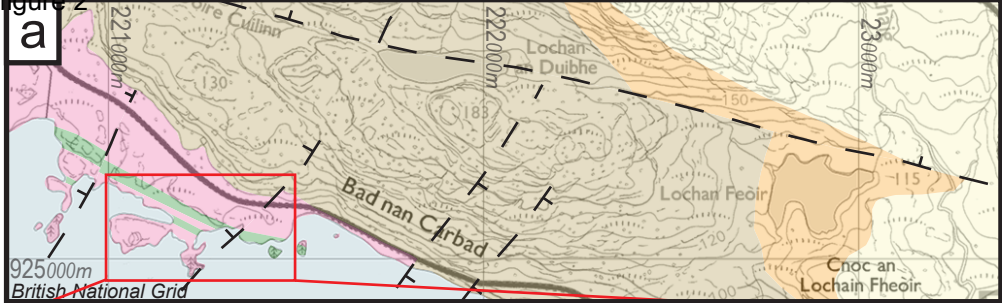


figure 3

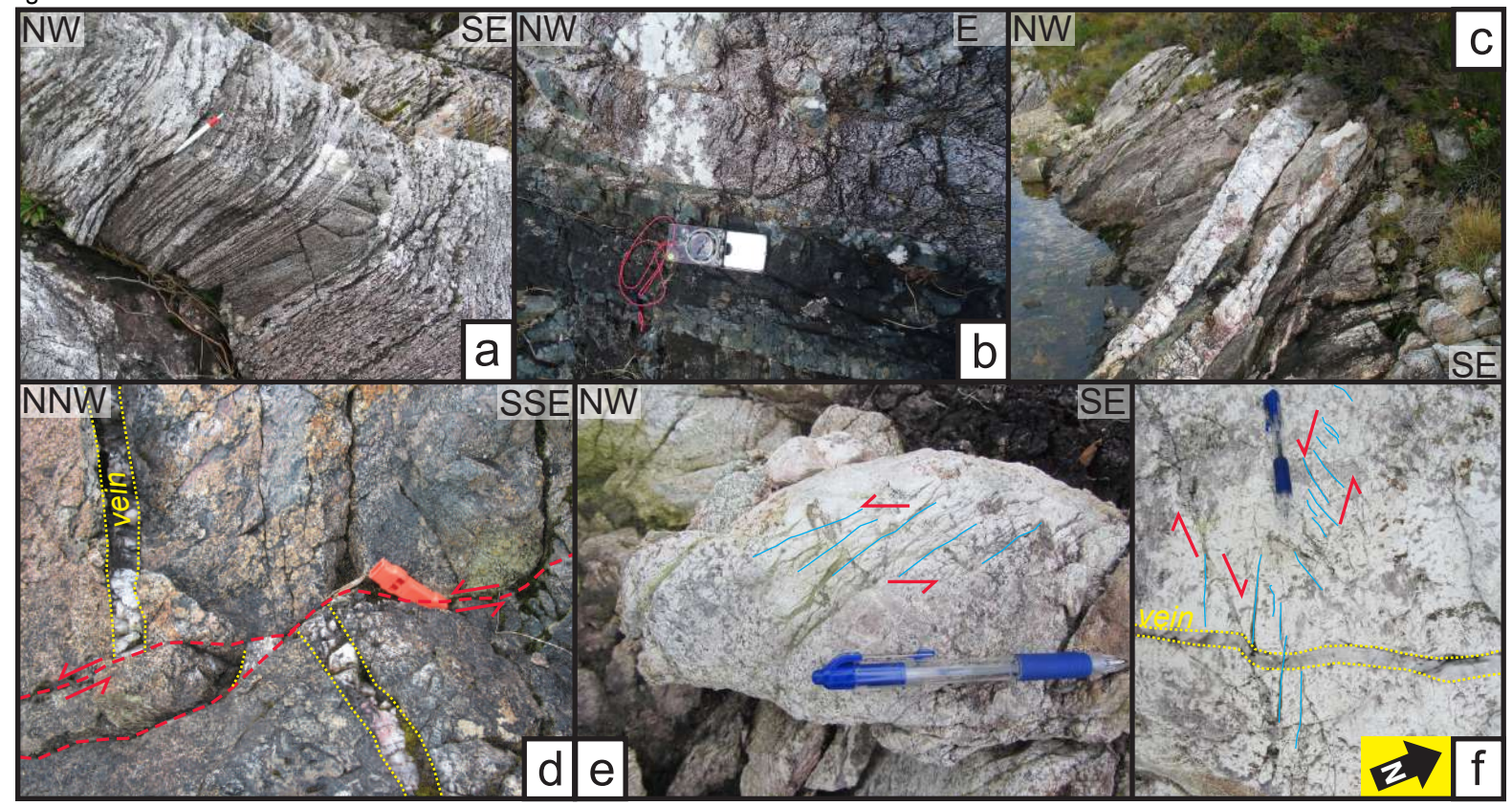


Figure 4

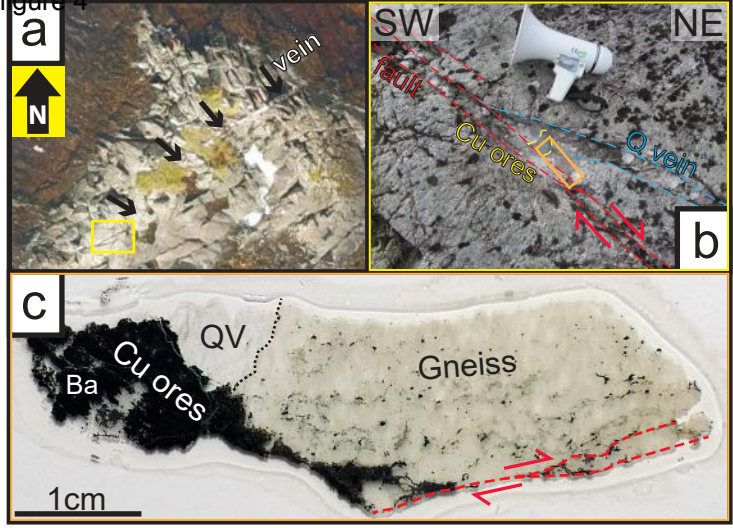


figure 5

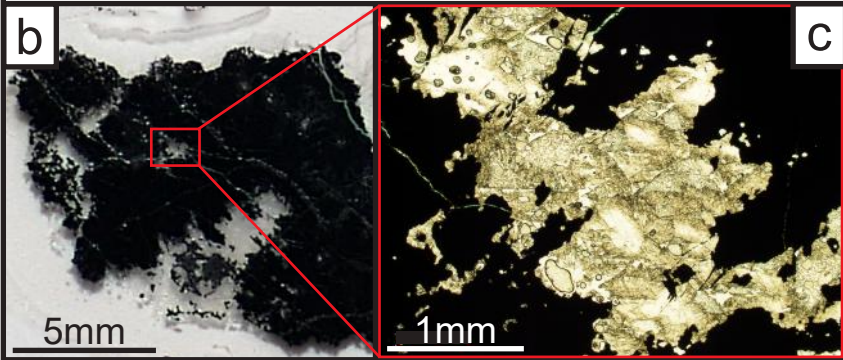
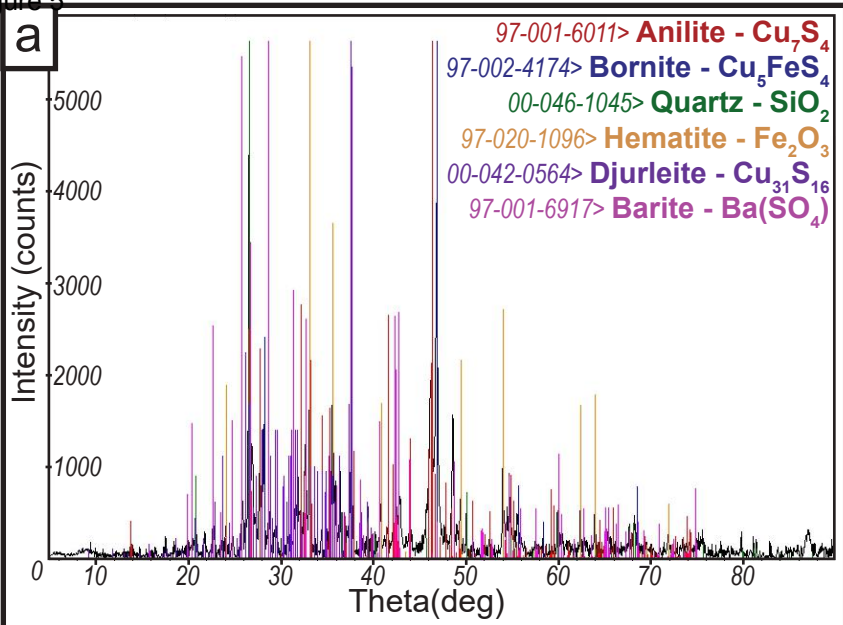


figure 6

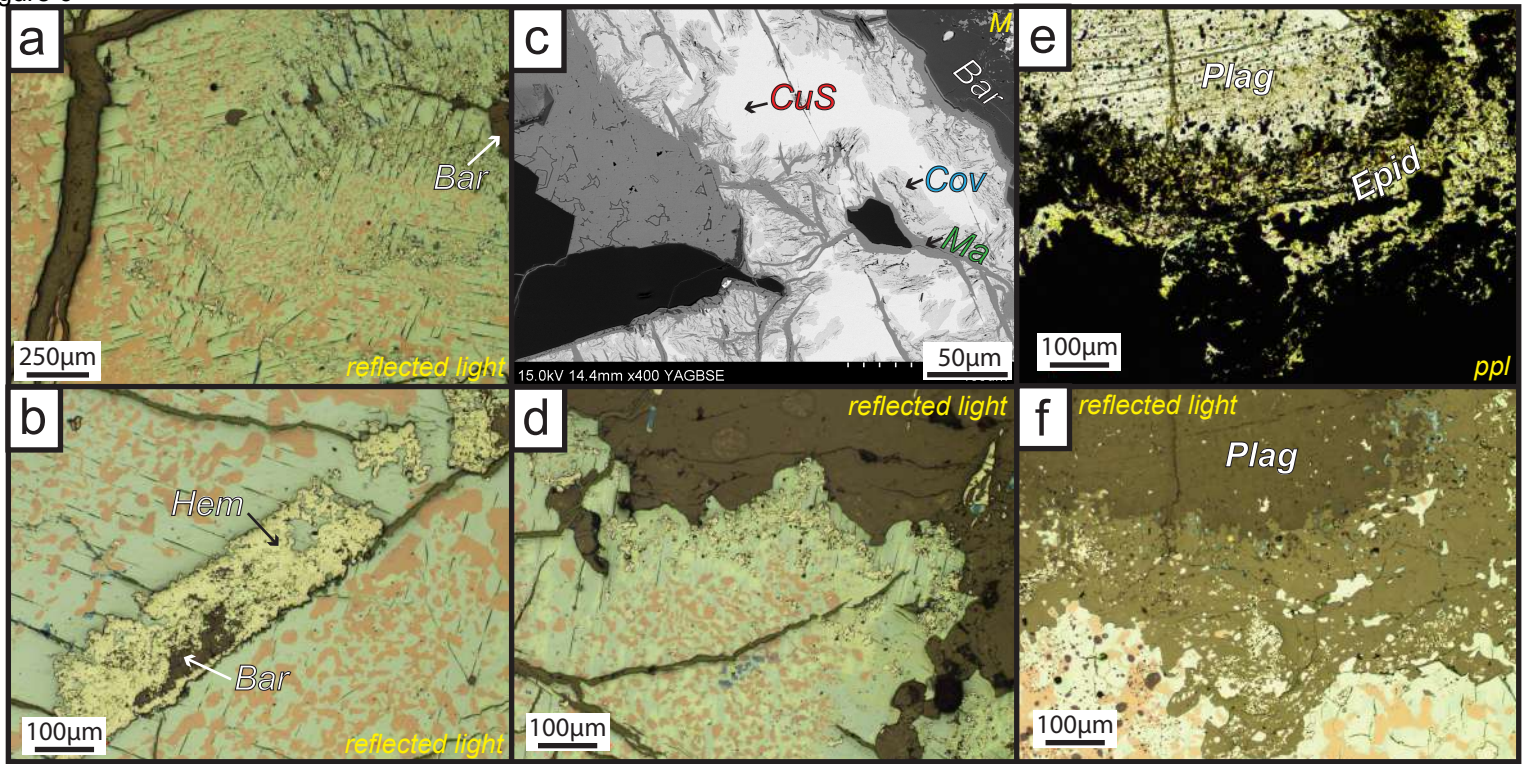


Figure 7

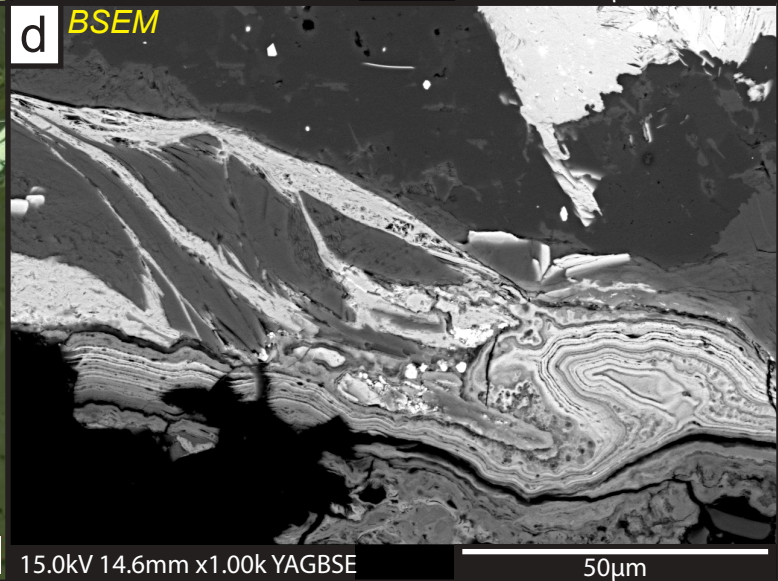
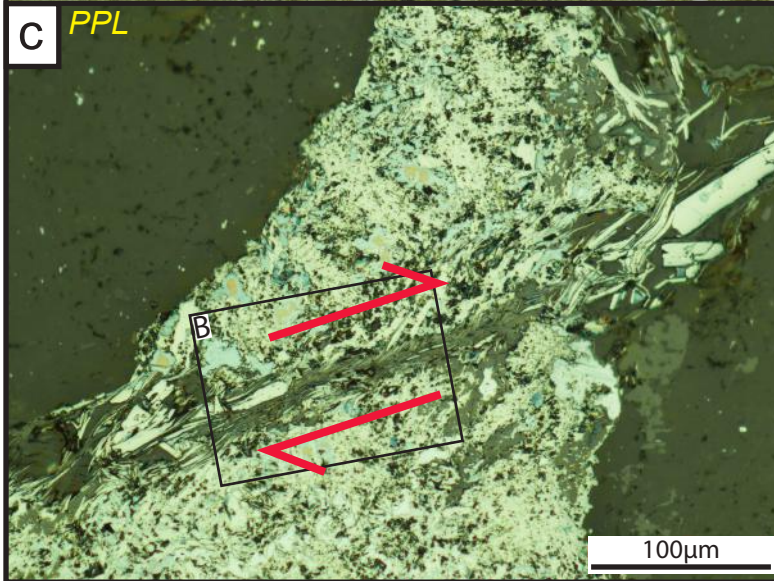
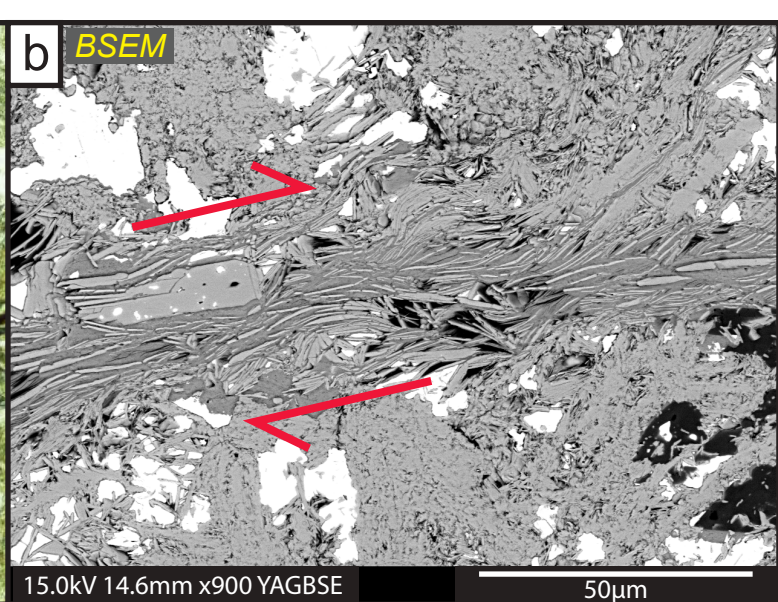
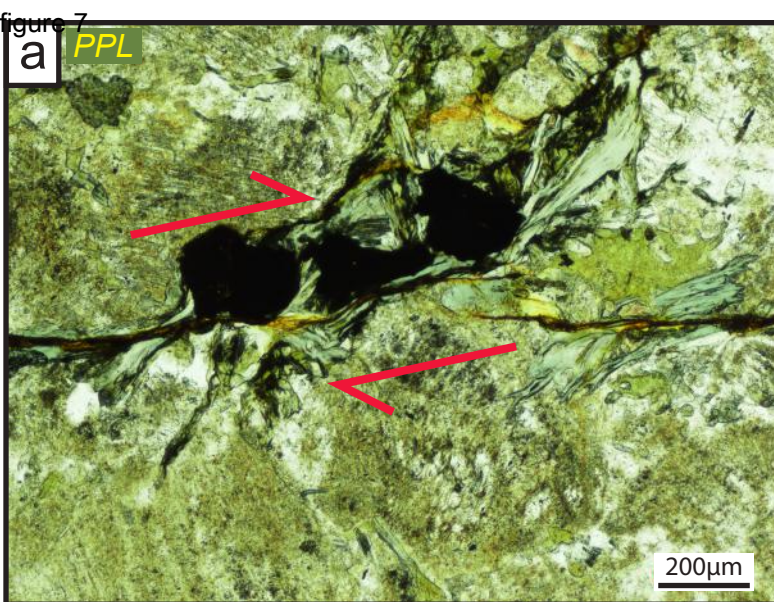
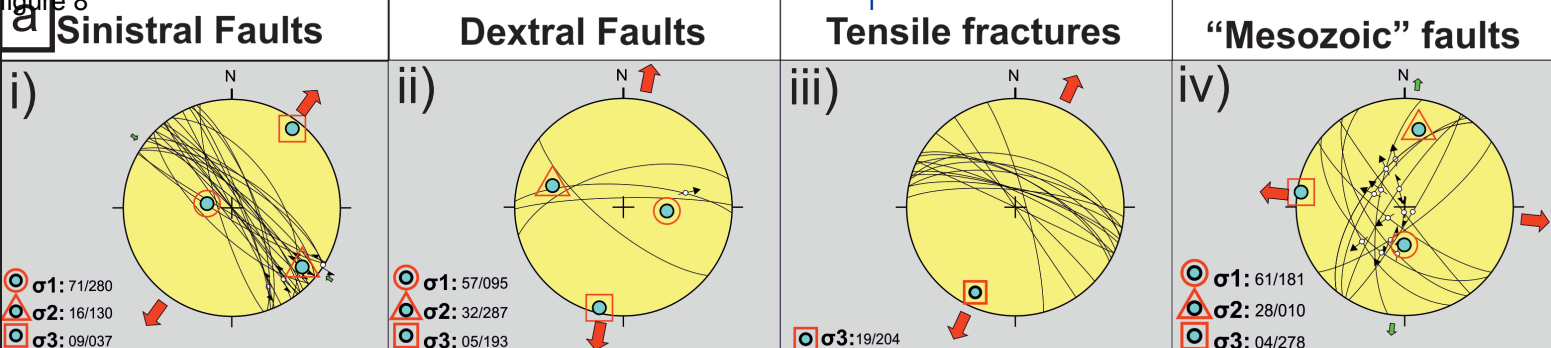


Figure 8



Confidence weighted stress inversion of all Sinistral + Dextral shear fractures

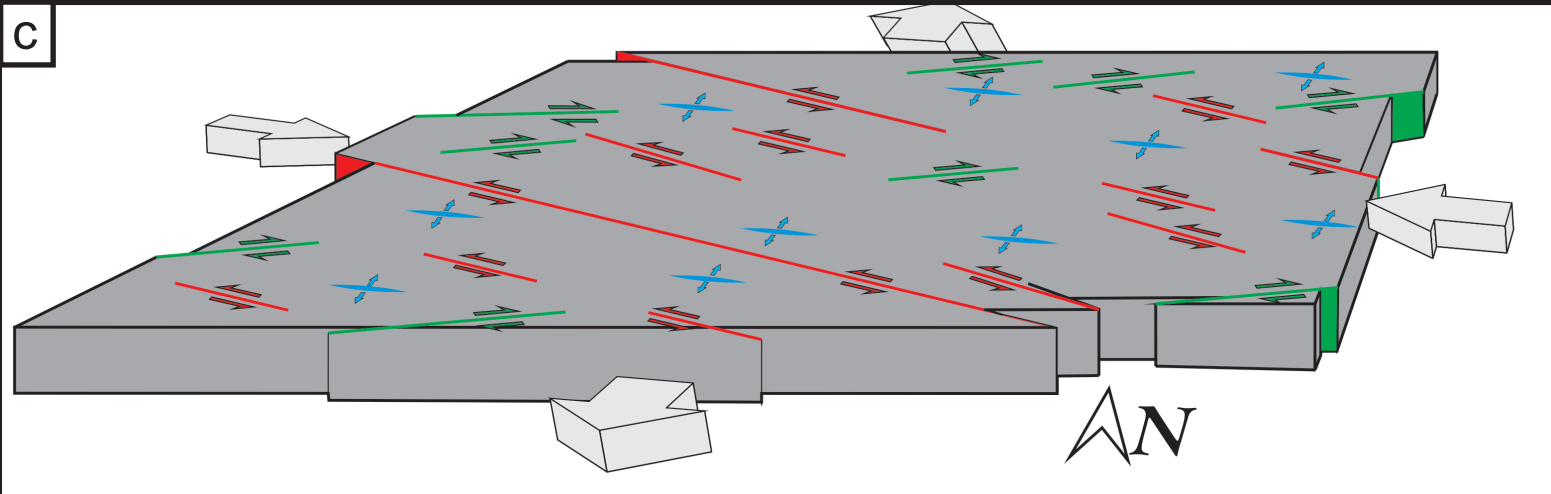
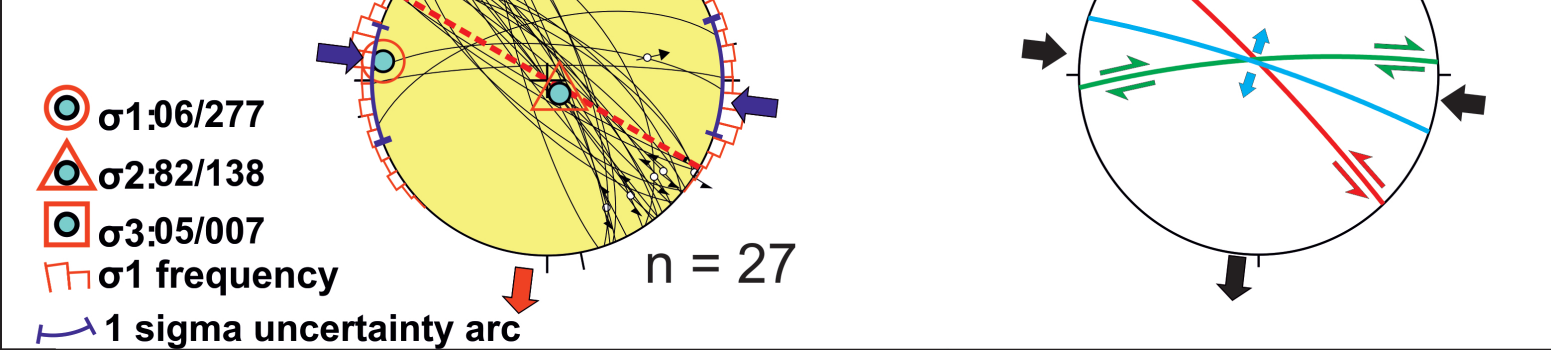


figure 9

